Physics of the Earth and Planetary Interiors 175 (2009) 106–114

Contents lists available at ScienceDirect

Physics of the Earth and Planetary Interiors

journal homepage: www.elsevier.com/locate/pepi

High-pressure infrared spectroscopy of the dense hydrous magnesium silicates phase D and phase E

Sean R. Shieh[a,*], Thomas S. Duffy[b], Zhenxian Liu[c], Eiji Ohtani[d]

[a] Department of Earth Sciences, University of Western Ontario, London, Ontario N6A 5B7, Canada
[b] Department of Geosciences, Princeton University, Princeton, NJ 08544, USA
[c] Geophysical Laboratory, Carnegie Institution of Washington, Washington, DC 20015, USA
[d] Department of Mineralogy, Tohoku University, Sendai 980-8578, Japan

ARTICLE INFO

Article history:
Received 4 August 2008
Received in revised form 20 January 2009
Accepted 3 February 2009

Keywords:
Phase D
Phase E
Infrared spectroscopy
High-pressure
Hydrous phases

ABSTRACT

Phases D and E are hydrous magnesium silicates that are stable at high-pressure–temperature conditions and could serve as H_2O carriers in the Earth's mantle, especially in subducting slabs. Using synchrotron infrared (IR) spectroscopy, we measured the infrared spectra of polycrystalline samples of phases D and E to 42 and 41 GPa, respectively. For both phases, at least three broad OH stretch vibrations were observed at elevated pressures indicating that each phase has multiple hydrogen positions that exhibit disorder. No structural phase transition or amorphization was observed for either phase over the measured pressure range. The mode Grüneisen parameters of phases D and E are in the range of −0.12 to 1.14 and −0.17 to 0.83, respectively, with mean values of 0.41 (phase D) and 0.31 (phase E). Using empirical correlations of OH frequency and O···H and O···O bond lengths; the six OH vibrations of phase D at ambient pressure have corresponding O···H and O···O bond distances in the range of 1.519–1.946 Å and 2.225–2.817 Å, whereas the four OH vibrations of phase E have the corresponding O···H and O···O bond distances in the range of 1.572–2.693 Å and 2.557–2.986 Å. These ranges encompass values reported from single-crystal X-ray diffraction measurements. At high pressures, the observable OH stretching vibrations exhibit both positive and negative pressure slopes. Our high-pressure infrared spectra for phase D do not support the occurrence of hydrogen symmetrization as predicted by first-principles calculations.

1. Introduction

Hydrogen is a geochemically important element whose abundance is poorly constrained in the Earth's deep interior (Jacobsen and van der Lee, 2006). The presence of hydrogen even in small quantities can affect phase relations, melting temperature, rheology, and other key properties of the deep Earth (e.g., Wood and Corgne, 2007; Williams and Hemley, 2001). Dense hydrous magnesium silicates (so-called alphabet phases) are a class of hydrous silicates that form under high-pressure–temperature conditions in the $MgO–SiO_2–H_2O$ system (Williams and Hemley, 2001; Smyth, 2006). These silicates are potentially important components of the deep Earth water cycle especially in cold slab environments (e.g., Liu, 1986, 1987; Kanzaki, 1991; Shieh et al., 1998; Frost, 1999; Kawamoto, 2004; Ohtani et al., 2004; Komabayashi and Omori, 2006). In particular, phase E is likely to be an important water carrier near the base of the upper mantle and the transition zone (Stalder and Ulmer, 2001; Litasov and Ohtani, 2003). Phase D may be the major H_2O-bearing phase at the top of the lower mantle in low-temperature slab environments for peridotite compositions (Ohtani et al., 2001, 2004; Komabayashi and Omori, 2006).

High-pressure measurements of vibrational spectra of phases D and E have proven to be challenging. Williams (1992) observed two weak modes in the OH stretching region of the infrared (IR) spectrum from a sample of pyroxene and water that had been laser heated at 32–34 GPa, possibly producing phase D. At ambient pressure, Raman spectra of phase D have been reported by Liu et al. (1998), Frost and Fei (1998), Ohtani et al. (1997), and Xue et al. (2008). For phase E, Raman spectra have been reported at ambient pressures in several studies (Mernagh and Liu, 1998; Frost and Fei, 1998; Shieh et al., 2000a,b) and at high pressures up to 19 GPa by Kleppe et al. (2001). For the IR measurement of phase E, only very weak ambient pressure spectra have been reported to date (Mernagh and Liu, 1998).

Phase E has the ideal formula of $Mg_2SiO_2(OH)_4$ but is highly disordered and exhibits variable Mg/Si ratios and hydrogen contents. The phase has rhombohedral symmetry ($R\bar{3}m$) with Si in tetrahedral and Mg in octahedral coordination; the MgO_6 octahedra form brucite-type layers cross-linked by a layer with a mixture of MgO_6 octahedra, SiO_4 tetrahedra and vacancies (Kudoh et al., 1993). All

* Corresponding author. Tel.: +1 519 850 2467; fax: +1 519 661 3198.
E-mail address: sshieh@uwo.ca (S.R. Shieh).

0031-9201/$ – see front matter © 2009 Elsevier B.V. All rights reserved.
doi:10.1016/j.pepi.2009.02.002

oxygens are equivalent but there are two distinct Mg octahedra and the Si tetrahedron is highly distorted. The structure lacks long-range order. Charge balance is maintained locally by protonation, and a range of Mg/Si ratios and hydrogen contents can be found in phase E.

Phase E can be synthesized from hydrous olivine and serpentine at 13–17 GPa and high temperature (Shieh and Ming, 1996; Irifune et al., 1998; Stalder and Ulmer, 2001). Powder X-ray diffraction studies show that it remains crystalline to at least 42 GPa (Shieh and Duffy, 2003; Shieh et al., 2000a,b). Raman spectra at ambient pressure show broad peaks, consistent with considerable structural disorder (Frost and Fei, 1998; Kleppe et al., 2001). Raman measurements reported three OH vibrations at 2492, 3429, and 3617 cm^{-1}, but the mode at 2492 cm^{-1} could only be detected at ambient conditions (Kleppe et al., 2001). The OH mode at 3429 cm^{-1} broadened with pressure and reached a peak width twice its initial value at pressure of 19 GPa.

Phase D has an ideal formula of $MgSi_2O_4(OH)_2$ and crystallizes in the trigonal system (space group $P\bar{3}1m$). This phase is also disordered with variable Mg/Si ratios and hydrogen contents of 10–18 wt% H_2O (Yang et al., 1997). Ambient-pressure Raman spectra show broad peaks for both lattice and OH modes (Ohtani et al., 1997; Frost and Fei, 1998). Phase D has all silicon in octahedral coordination and is stable to 70 GPa at room temperature (Frost and Fei, 1998; Shieh, unpublished data).

The structure consists of alternating layers of MgO_6 and SiO_6 octahedra stacked along the c direction. In the SiO_6 layers, the octahedra share edges forming brucite-like layers but 1/3 of the octahedral sites are vacant. The MgO_6 octahedra are oriented above and below the vacant sites and share corners with SiO_6 octahedra. Two-thirds of the sites are vacant in the Mg octahedral layer. The SiO_6 octahedra are distorted as the O–O distance along the shared edge is much shorter than those along the unshared edges (Yang et al., 1997), and this is supported by recent NMR spectroscopy measurements (Xue et al., 2008). The MgO_6 octahedra show little distortion.

Synthesized phase D samples have Mg/Si ratios ranging from about 0.55 to 0.71 indicating excess Mg and/or deficient Si. Based on recent NMR data, it is proposed that there are both Si vacancies and substitution of Mg into Si sites (Xue et al., 2008) with H providing charge balance. The partially occupied disordered H bond positions are proposed to be located within the Mg octahedral layer and bonded to oxygens of the Si octahedra (Yang et al., 1997; Xue et al., 2008). Phase D is the same phase as the other reported hydrous phases G and F (Ohtani et al., 1997; Kanzaki, 1991), although the Mg/Si ratio and H_2O content vary with synthesis conditions.

Infrared spectroscopy using a synchrotron source is a powerful tool for studying hydrogen-bearing materials at high pressures. Such studies provide insights into phase stability and hydrogen bonding and their pressure dependence. Vibrational spectra also provide insights into thermodynamic properties such as entropy, heat capacity, and thermal expansivity through modeling the contribution of vibrational frequencies to these quantities (e.g., Cynn et al., 1996). In this study, we used high-pressure synchrotron infrared spectroscopy to investigate both phases E and D to pressures above 40 GPa.

2. Experimental method

Phase D was synthesized from a 2:1 mixture of $SiO_2 + Mg(OH)_2$ sealed in a welded platinum capsule at 20 GPa and ~1000 °C for about 3 h in a multi-anvil apparatus at Tohoku University. The sample was examined by X-ray powder diffraction and confirmed to be pure phase D. The lattice parameters are: $a = 4.756(3)$ Å and $c = 4.345(4)$ Å. These values are similar to earlier reports (Ohtani et al., 1997; Yang et al., 1997) from samples whose chemical composition ranged from $Mg_{1.11}Si_{1.89}H_{2.22}O_6$ (Yang et al., 1997) to $Mg_{1.84}Si_{1.73}H_{2.81}O_6$ (Ohtani et al., 1997). Phase E was obtained from the same batch used for a previous X-ray diffraction study (Shieh et al., 2000a). It was synthesized in a Walker-type multi-anvil press at the Geophysical Laboratory of the Carnegie Institution of Washington using a 1:2 mixture of $SiO_2 + Mg(OH)_2$ compressed to 14.5 GPa and heated to 1000 °C. The chemical composition determined by electron probe microanalysis is $Mg_{2.23}Si_{1.18}H_{2.80}O_6$ and the lattice parameters are: $a = 2.9653(5)$ Å and $c = 13.890(4)$ Å (Shieh et al., 2000a).

Phases D and E samples were first examined by infrared spectroscopy at ambient conditions by placing powdered samples on top of a diamond anvil (D and E) or a KBr substrate (D). Further measurements were then performed at high pressures in a diamond anvil cell. The high-pressure cells used natural type IIa diamonds with 400-μm diameter culets. The samples were prepared by crushing the small single crystals into polycrystalline foils on diamond anvils without further grinding. The foils were loaded into a ~100-μm diameter gasket hole such that they filled less than 50% of the sample chamber volume and were confined entirely within one-half of the hole. This arrangement allowed background measurements to be performed from the other side of the hole without contamination from the sample. KBr powder, serving as a pressure medium, was used to fill the empty part of the sample chamber and to cover the sample. Small ruby balls were placed near the center and edge of the sample chamber for pressure determination (Mao et al., 1978).

High-pressure infrared (IR) spectra were collected at beamline U2A of the National Synchrotron Light Source. The synchrotron IR beam was focused by a nitrogen gas purged microscope (Bruker IRscope II) and a 30 μm × 40 μm aperture was used during the experiment. Experiments were performed solely in transmission mode and the mid-IR (400–4000 cm^{-1}) signal was collected using a Bruker IFS 66v/S FTIR spectrometer and a liquid nitrogen-cooled MCT detector with a resolution of 4 cm^{-1}, which corresponds to an uncertainty of 0.015 Å near 3600 cm^{-1}. At each pressure, the final IR absorption spectrum was obtained by subtracting the background spectrum from the sample spectrum. Pressures were measured before and after each IR measurement, and the pressure difference was generally less than 1 GPa. The pressures measured from ruby positions near the center and edge showed differences of ~0.5 GPa at 13 GPa, ~1 GPa at 25 GPa and ~2 GPa at 40 GPa. Only the pressures recorded after IR measurements are reported in this study. Special care was taken to avoid the contamination of our IR measurements by ruby grains. Data processing was carried out using the Peakfit program and the spectral data were fitted to a combined Gaussian–Lorentzian profile function.

3. Results

3.1. Phase D

The infrared spectrum of phase D measured at ambient conditions showed 13 observable modes (Fig. 1). To clarify potential ambiguity arising from the contamination by diamond at 2000–2500 cm^{-1}, phase D samples were examined on diamond and KBr substrates. The peak at 1604 cm^{-1} was assigned as the H–O–H-bending vibrational mode. The peaks at 2102 and 2240 cm^{-1} may be strong H bonds of phase D but they were obscured at high pressures by interference with diamond. Ten modes attributable to phase D at elevated pressures were found in this study (Table 1). There are four modes between 656 and 836 cm^{-1} as well as modes at 1044 and 1217 cm^{-1}. At frequencies below 2000 cm^{-1}, the Raman spectrum of phase D shows a broadly similar pattern that features a group of peaks in the 600–800 cm^{-1} region with additional modes at 1078 and 1269 cm^{-1} (Frost and Fei, 1998; Xue et al., 2008). Possi-

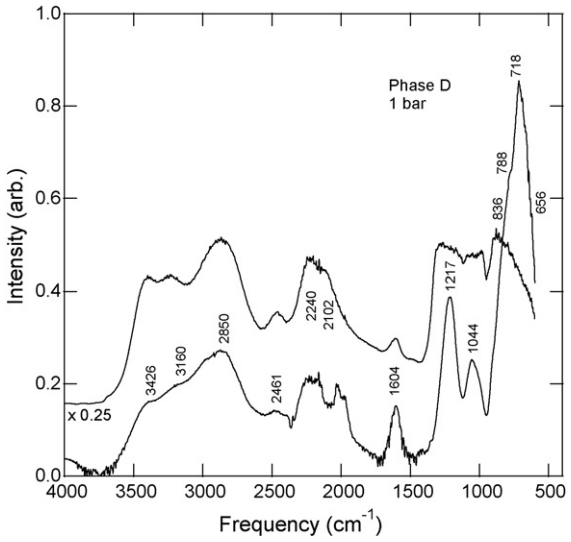

Fig. 1. The infrared spectra of phase D at ambient conditions: (top spectrum) phase D on a KBr substrate and (bottom spectrum) phase D on a diamond anvil.

ble assignments of modes can be made by systematic comparison with other phases, especially hydrous silicates and consideration of frequencies and intensities.

The two lowest frequency modes for phase D may be associated with bending of Si–O octahedra as inferred from studies of phase B and superhydrous phase B (Cynn et al., 1996). The weak pressure dependence (discussed below) of the 656 cm^{-1} mode suggests it could have a different origin from the other modes. An alternative possibility for this mode is an M–O–H bending mode, as these modes often have lower pressure slopes (Williams and Guenther, 1996). Modes in the range of ~800–1100 cm^{-1} region may be associated with internal stretching modes of SiO_6 octahedra (Cynn et al., 1996). The origin of the IR and Raman modes in the 1200–1300 cm^{-1} range is less clear and includes the possibility of an overtone, an LO mode, or an O–H···O bending vibration.

In this study we observe as many as six OH stretching modes (2102, 2240, 2461, 2850, 3160, and 3426 cm^{-1}) for phase D (and four at elevated pressures). This differs from some previous Raman measurements which detected only a single broad OH stretching peak near 2850 cm^{-1} (Ohtani et al., 1997; Frost and Fei, 1998). However, the Raman spectrum of Frost and Fei (1998) shows a possible weak peak near 2500 cm^{-1}. Also the 2850 cm^{-1} mode is asymmetric, suggesting the presence of an additional mode at higher frequency. Xue et al. (2008) recently reported weak phase D Raman spectra showing three peaks at 2240, 2470, and 2810 cm^{-1}. These correspond closely to three of the peaks in our ambient-pressure IR spectra (2240, 2461, and 2850 cm^{-1}). Thus, in fact, the Raman and IR spectra of phase D actually show similarities. Our highest frequency OH band at 3426 cm^{-1} is somewhat different from previous IR measurement of a laser-heated pyroxene and H_2O sample that reported modes at 3270 and 3352 cm^{-1} (Williams, 1992) but the identification of this synthesis product as phase D is questionable.

All the OH modes we observed are broad, and the full width at half maxima (FWHM) for the peaks between 2850 and 3426 cm^{-1} are in the range of 260–440 cm^{-1}, indicative of disorder in the H positions. H disorder is also supported by a single-crystal X-ray diffraction study (Yang et al., 1997) and NMR spectroscopy measurements (Xue et al., 2008).

The phase D sample was gradually compressed at steps of 1–2 GPa to about 42 GPa. Fig. 2a and b shows that the evolution of the infrared spectra with pressure. Most of the features of phase D can be readily observed to the highest pressure. Thus, in contrast to a previous report (Liu et al., 1998), no phase transformation or amorphization was found to at least 42 GPa. The 1044 cm^{-1} band disappears at pressure greater than 28 GPa. However, the band at 1217 cm^{-1} remained observable to 42 GPa. The OH bands became weaker at higher pressures and this may be partially attributed to thinning of the sample.

Figs. 3 and 4 show the variation of frequency shifts of vibrational modes of phase D with pressures. The internal modes mostly increase with similar slopes except for the mode at 656 cm^{-1} which exhibits a lower slope (Fig. 3 and Table 1). The 1217 cm^{-1} band is the only one with a non-linear trend and it becomes pressure-independent above 30 GPa. For the OH bands, the 3160 and 3426 cm^{-1} bands have negative slopes of −0.57 and −2.08 cm^{-1}/GPa, respectively, whereas the 2850 cm^{-1} band has a positive slope. The slope of the 3426 cm^{-1} band is about 3.5 times as steep as that of the 3160 cm^{-1} band. The weak OH band at 2461 cm^{-1} could be due to the unique structure of phase D with highly distorted SiO_6 and it remained observable at high pressures.

The mode Grüneisen parameters, γ_{i0}, of phase D (Table 1) were obtained from the following equation:

$$\gamma_{i0} = \frac{K_{T0}}{\nu_{i0}} \times \left(\frac{\partial \nu_i}{\partial P}\right)_0 \quad (1)$$

where K_{T0} is the zero-pressure isothermal bulk modulus (166 GPa; Frost and Fei, 1999), ν_{i0} is the frequency of the ith band at ambient conditions, and $(\partial \nu_i/\partial P)_0$ is the measured slope of mode, i, at ambient conditions. Note that the γ_{i0} values for phase D are mostly less than 1, which are typical for hydrous phases (e.g., Hofmeister et al., 1999). The unweighted average Grüneisen parameter from all the observed IR modes is 0.41.

Table 1
Infrared vibrational frequencies and mode Grüneisen parameters of phase D.

ν_{i0} (cm^{-1})	dν_i/dP (cm^{-1}/GPa)	γ_{i0}
656	0.84	0.21
718	2.24	0.52
788	3.10	0.65
836	3.23	0.64
1044	4.55	0.72
1217	8.34	1.14
2461	3.53	0.24
2850	2.31	0.13
3160	−0.57	−0.03
3426	−2.08	−0.12

3.2. Phase E

Over the mid-IR (400–4000 cm^{-1}) measurement range, the infrared spectrum of phase E showed four low-frequency peaks (663, 801, 955, and 1037 cm^{-1}) and four OH stretching modes (2455, 2988, 3411, and 3638 cm^{-1}) at ambient conditions (Fig. 5). Two of the mid-IR modes (663 and 955 cm^{-1}) occur at similar locations to values from previous Raman measurements (Frost and Fei, 1998; Kleppe et al., 2001). The lowest-frequency modes are likely due to internal stretching modes of the SiO_4 tetrahedra (Cynn et al., 1996; Kleppe et al., 2001). The band at 1037 cm^{-1} is similar to that observed for phase D (i.e., 1044 cm^{-1}) and may have a similar origin. At frequencies less than 1200 cm^{-1}, the internal bands of phase E have FWHM in the range of 50–130 cm^{-1}, which are comparable to but slightly broader than those observed in Raman data (i.e., 55–100 cm^{-1}). These features of the internal modes of phase E may be attributed to the short-range order of the structure and distorted SiO_4 tetrahedron (Kudoh et al., 1993).

The peak positions at 2455, 3411, and 3638 cm^{-1} are all similar to the peak locations in Raman measurements (2492, 3331–3429 cm^{-1}, and 3613–3631 cm^{-1} for phase E) (Ohtani et al.,

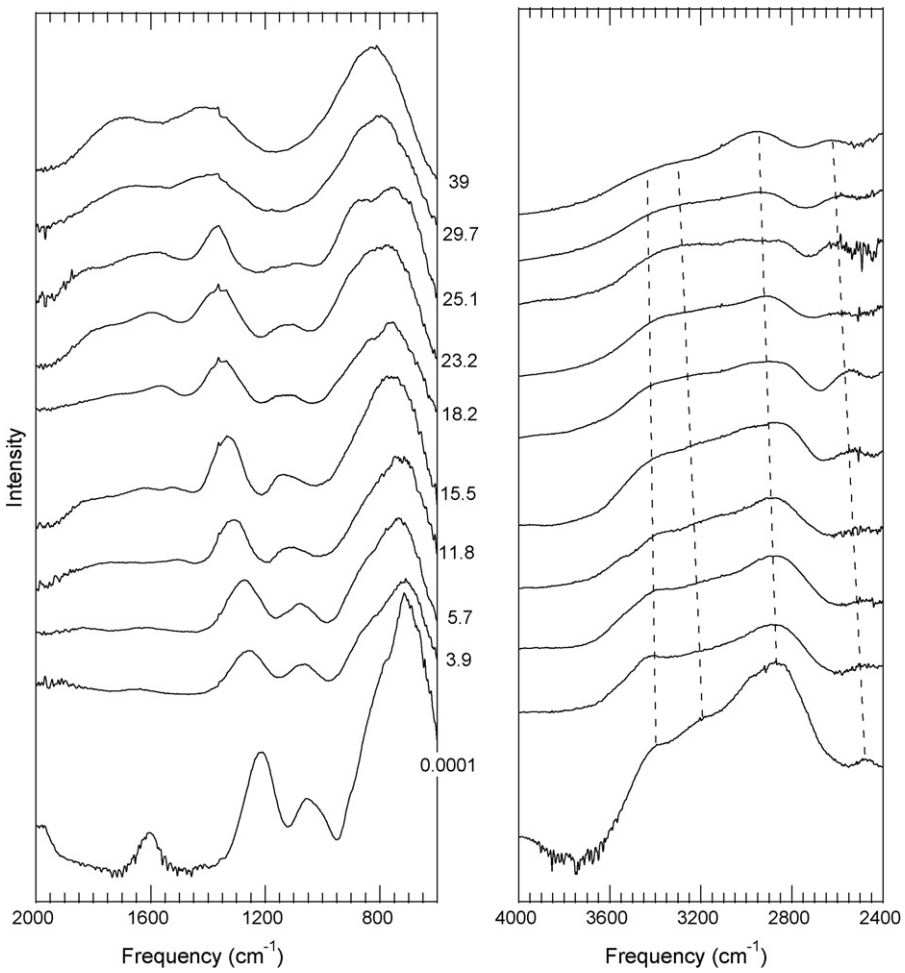

Fig. 2. Representative spectra of phase D under compression to 39 GPa. The pressure (in GPa) is labeled on the right side of the left panel: (a) internal modes and (b) OH stretching modes. Dashed lines are guides for the eye.

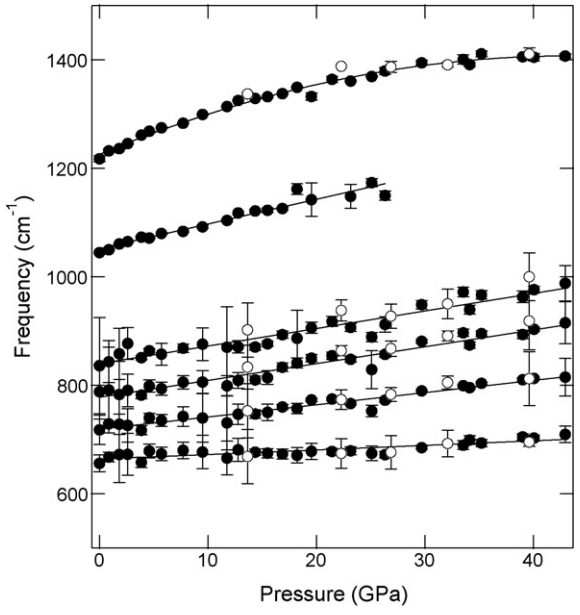

Fig. 3. The frequency shifts of internal modes as a function of pressure for phase D. The solid curves are either linear or second-order polynomial fits to the data. Solid symbols were obtained during compression and open symbols were obtained during decompression.

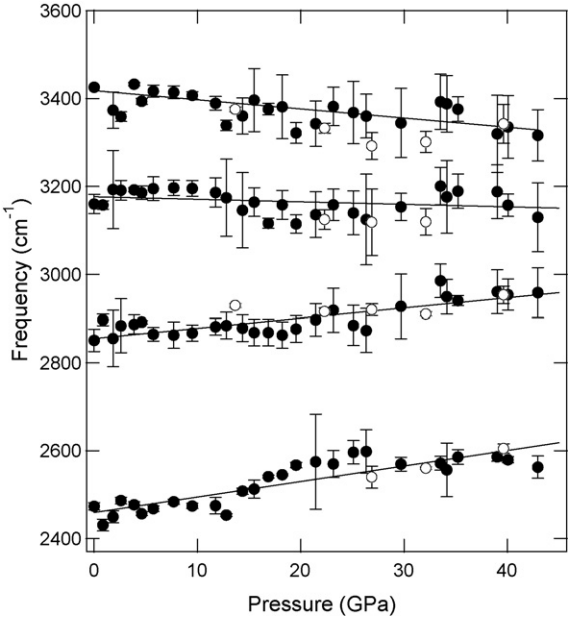

Fig. 4. The frequency shifts of OH vibrational modes as a function of pressure for phase D. The solid lines are linear fits to the data. Solid symbols were obtained during compression and open symbols were obtained during decompression.

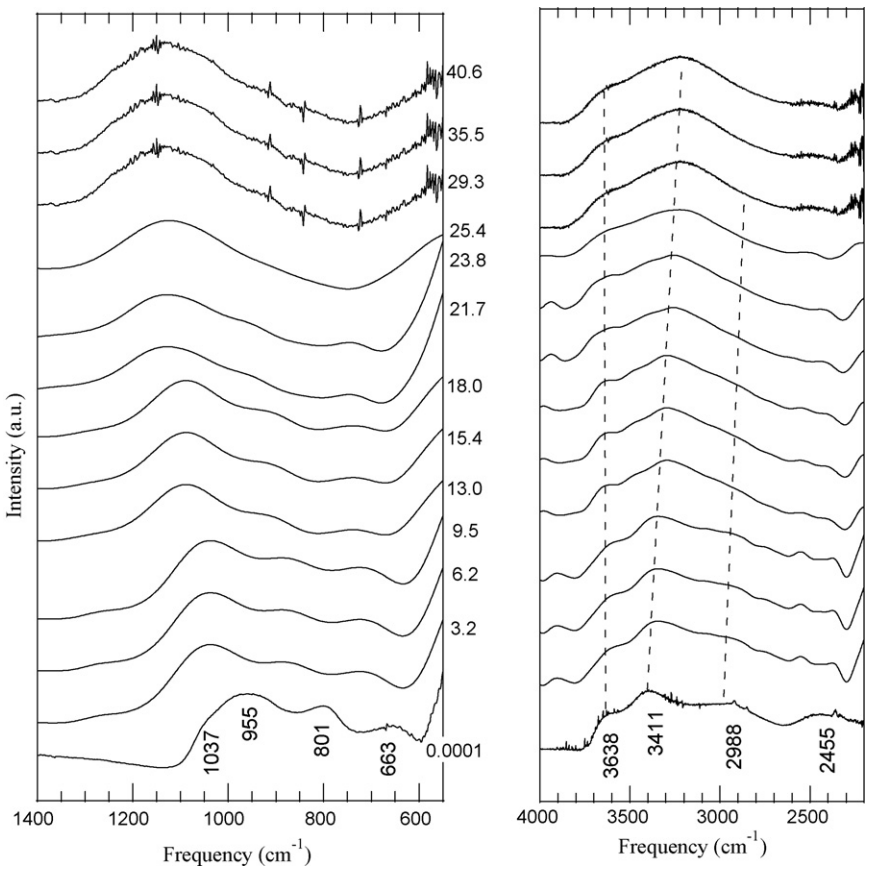

Fig. 5. Representative IR spectra of phase E under compression to 40.6 GPa. The frequency (in wavenumbers) at 1 bar is denoted next to each peak. The pressure (in GPa) is labeled on the right hand side of the left panel: (a) internal modes and (b) OH stretching modes. Dashed lines are guides for the eye.

1995; Frost and Fei, 1998; Mernagh and Liu, 1998; Shieh et al., 2000a; Kleppe et al., 2001), but the band at 2988 cm^{-1} was not observed in previous studies. The OH stretching peaks are generally broad, and peak fits to the ambient pressure data yield FWHM of the three bands at 2988, 3411, and 3638 cm^{-1} that are about 560, 350, and 120 cm^{-1}, respectively. The highest frequency OH vibration of phase E found from the Raman measurement (Kleppe et al., 2001) has a similar width as our IR data (125 cm^{-1} vs. 120 cm^{-1}) and it is sharper than other OH peaks. This peak therefore may originate from a more ordered proton position, compared to the lower frequency OH vibrations. The expected frequency of the fundamental free OH^- ion vibrations is about 3555 cm^{-1} (Lutz, 1995), and this is lower than that of phase E at 3638 cm^{-1}. Similar high frequency bands are characteristic of some of the dense magnesium silicates and can be also found for chondrodite (3687 cm^{-1}), phase B (3611 and 3630 cm^{-1}) and superhydrous phase B (3696 cm^{-1}) (Cynn et al., 1996), while the highest frequency band for phase D is 3426 cm^{-1}.

Phase E was compressed to 40.6 GPa and spectra at more than 20 different pressures were recorded. The four low-frequency modes were identifiable at pressure to ~24 GPa, but became difficult to distinguish at higher pressures (Fig. 5). These Si–O stretching peaks tend to merge into a single broad peak together with weak shoulders at pressure greater than 25 GPa. The OH stretching modes at 2988–3638 cm^{-1} remained detectable to about 41 GPa but appear as a broad peak centered at ~3200 cm^{-1} with weak shoulders.

Fig. 6 shows that the frequency shifts of the low-frequency modes (663–1036 cm^{-1}) of phase E display similar slopes as a function of pressure, indicating the similar responses of Si–O stretching modes with increasing pressures. Note that at pressure below 5 GPa the frequency shifts of the internal modes appear to deviate from linear trends. The IR bands of phase E in general have more positive slopes, ranging from 5.44 to 6.05 cm^{-1}/GPa, compared to the Raman data (3.0–4.2 cm^{-1}/GPa) (Kleppe et al., 2001). The slopes are also steeper than those of phase D (0.84–3.23 cm^{-1}/GPa) at comparable frequencies, consistent with the greater compressibility of phase E relative to phase D.

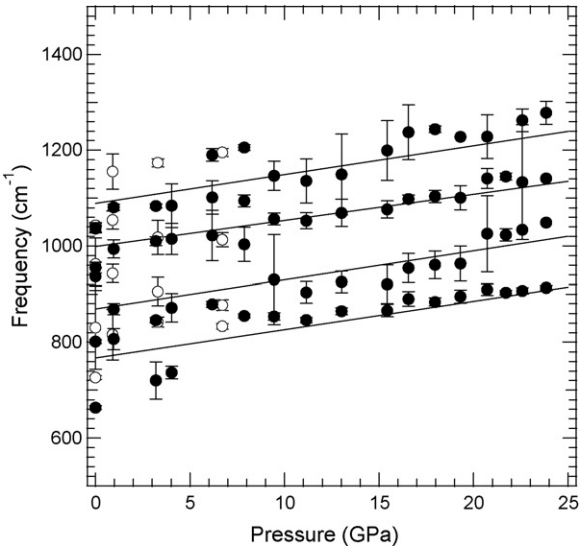

Fig. 6. The frequency shifts of internal modes as a function of pressure for phase E. The solid lines are linear fits to the data. Solid symbols were obtained during compression and open symbols were obtained during decompression.

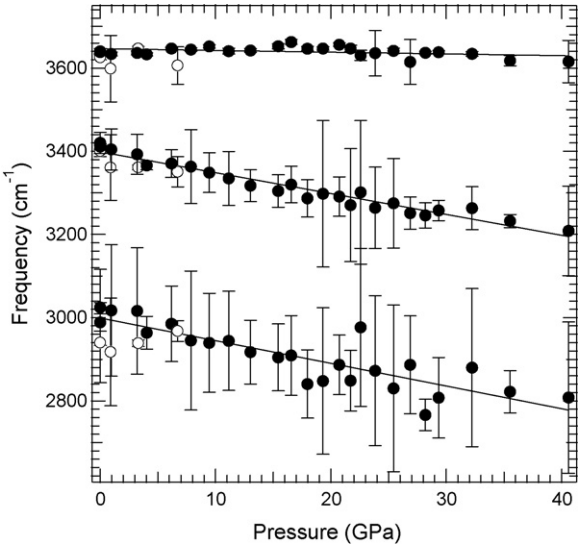

Fig. 7. The frequency shifts of OH vibrational modes as a function of pressure for phase E. The solid lines are linear fits to the data. Solid symbols were obtained during compression and open symbols were obtained during decompression.

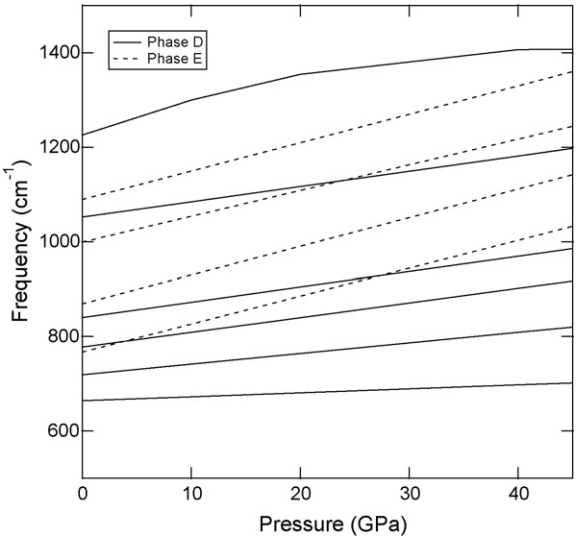

Fig. 8. Comparison of the frequency shifts of internal modes as a function of pressure for phases D and E.

The OH stretching modes at 2988 and 3411 cm^{-1} exhibit negative slopes, −5.45 and −5.01 cm^{-1}/GPa, respectively, whereas the 3638 cm^{-1} band has a weakly negative slope, −0.41 cm^{-1}/GPa (Fig. 7). The former two bands have more strongly negative frequency shifts with pressure than many other dense hydrous silicates (Hofmeister et al., 1999), and the slope for the 3411 cm^{-1} band is comparable to that observed for a band at 3429 cm^{-1} in Raman data (Kleppe et al., 2001). No band corresponding to the 2988 cm^{-1} peak was observed in Raman data. The highest frequency OH stretching mode of phase E has a near-zero positive slope which is also consistent with the slightly positive slope (0.49 cm^{-1}/GPa) for a mode at 3617 cm^{-1} observed in Raman spectra for this material (Kleppe et al., 2001).

The mode Grüneisen parameters (γ_{i0}) of phase E obtained from this study were calculated using Eq. (1) with a bulk modulus of 93 GPa (Shieh et al., 2000a) (Table 2). The internal Si–O modes of phase E at 663–1036 cm^{-1} have γ_{i0} values in a narrow range, 0.53–0.83, which are slightly higher than those found from Raman measurements (Kleppe et al., 2001). For the OH bands, the calculated γ_{i0} values are in the range of −0.17 to 0.06, which is in the range of those of other dense hydrous silicates (Hofmeister et al., 1999). An unweighted average Grüneisen parameter from all observed Raman (Kleppe et al., 2001) and IR modes (17 totals) is 0.31.

3.3. Comparison of phases D and E

Structurally, both phases D and E contain MgO_6 octahedral layers as part of their structures. The MgO_6 octahedra of phase D are isolated from each other whereas MgO_6 octahedra of phase E form brucite-type layers. Another major structural difference is that phase D possesses octahedrally coordinated silicon whereas phase E contains tetrahedrally coordinated silicon. However, the Si–O distances for the two materials are similar as phase D has six Si–O bonds with an averaged value at ~1.805–1.823 Å (Yang et al., 1997; Kudoh et al., 1997) while phase E has three Si–O bonds at 1.827–1.841 Å and one much shorter distance (1.661–1.675 Å) (Kudoh et al., 1993). The short Si–O distance of phase E is actually a normal distance for SiO_4 tetrahedron. Thus, the Si–O internal bands may occur at similar frequency ranges in both materials. Fig. 8 shows the comparison of the frequency shifts of internal modes of phases D and E. In general, modes of phase E have steeper slopes than those of phase D. For the bands with frequencies higher than 1000 cm^{-1}, phase D has higher frequency shifts than those of phase E whereas for those bands with frequencies lower than 900 cm^{-1}, phase E has slightly higher frequency shifts than those of phase D.

The frequency shifts of the OH bands reflect the character of the H-bonding and may correspond to the reduction of O···O distances with pressure. For phase D, both the 3160 and 3426 cm^{-1} bands have shallow negative slopes (Fig. 9) which may be asso-

Table 2
Infrared vibrational frequencies and mode Grüneisen parameters of phase E.

ν_{i0} (cm^{-1})	dν_i/dP (cm^{-1}/GPa)	γ_{i0}
663	5.89	0.83
801	6.05	0.70
955	5.42	0.53
1036	6.02	0.54
2455	–	–
2988	−5.45	−0.17
3411	−5.01	−0.14
3638	−0.41	−0.01

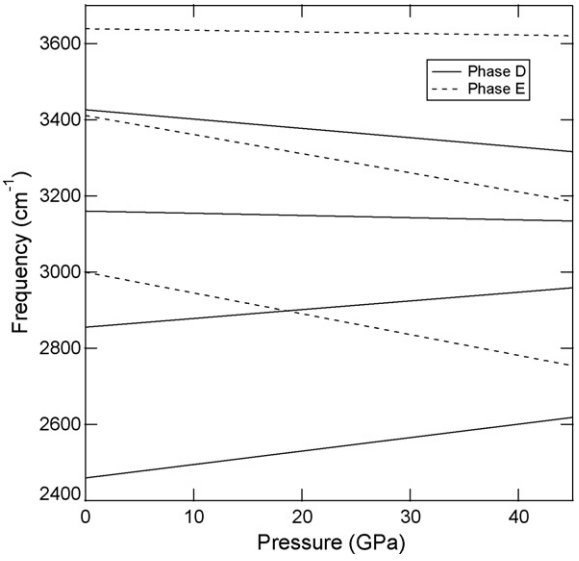

Fig. 9. Comparison of the frequency shifts of OH vibrational modes as a function of pressure for phases D and E.

ciated with the gradual shortening of O···O distances, as expected for an incompressible silicate such as phase D. Although the H positions of phase D occur in the vacancies of the MgO_6 layer (Yang et al., 1997), the SiO_6 octahedra share edges with each other and also share corners with MgO_6 octahedra and thus form a strong framework with alternating MgO_6 and SiO_6 octahedral layers along the *c*-axis. This results in a more incompressible structure. The relative compressibility with respect to layering may be reflected in the *c*/*a* ratio which initially decreases strongly with pressure but evolves to be nearly pressure independent above 20–25 GPa (Frost and Fei, 1998, Shieh et al., in preparation). A similar evolution of the *c*/*a* ratio is observed in highly anisotropic brucite-type hydroxides under compression (e.g., Duffy et al., 1995).

For phase E, the OH bands at 2898 and 3411 cm^{-1} have more negative slopes than those of phase D, while the 3638 cm^{-1} band exhibits a shallower slope (Fig. 9). Phase E (K_{0T} = 93 GPa) is more compressible than phase D (K_{0T} = 166 GPa) and the *c*/*a* ratio is largely independent of pressure for phase E (Shieh et al., 2000a). The presence of vacancies within the SiO_4 tetrahedra layers of phase E (Kudoh et al., 1993) may contribute to the strongly pressure-dependent frequency shifts of the OH modes of phase E.

The presence of multiple vibrational modes in the OH stretching region indicates that there are multiple H environments in phase E and phase D. For phase E, we observe four IR modes while three modes were observed by Raman spectroscopy (Kleppe et al., 2001). For phase D, we also observe a total of six modes ranging from 2102 to 3426 cm^{-1}. In contrast, a recent Raman study of phase D reported three modes spanning the frequency range 2240–2810 cm^{-1} (Xue et al., 2008).

Both positive and negative shifts of the OH modes are observed with pressure in this study. Negative shifts are typically associated with increased H bonding with compression as decreasing O···O distances result in lengthening of O–H bonds. Positive OH frequency shifts may be due to factors such as no or weak hydrogen bonding, repulsion by H^+ ions or other cations, reduction of hydrogen bonding due to changes in O–H···O angles, or O–H bond compression (Liu et al., 2003).

Based on its frequency, the band at 2850 cm^{-1} for phase D is regarded as a strong hydrogen bond whereas the band at 3638 cm^{-1} for phase E may have weak hydrogen bonding. At ambient pressure, the H···O and O···O bond distances in hydrous phases are known to be empirically correlated to the OH vibration frequency (Libowitzky, 1999). By adopting this correlation for our data, we can estimate bond distances and their changes as a function of pressure. We adopted Libowizky's regression function, $\nu = A - B \times \exp(-d/C)$ where A = 3622 cm^{-1}, $B = 238 \times 10^9$ cm^{-1}, C = 0.1346 Å for the O···O correlation, and A = 3632 cm^{-1}, $B = 1.79 \times 10^6$ cm^{-1}, C = 0.2146 Å for H···O correlation, respectively (Libowitzky, 1999). Based on this correlation, the H···O distance for the phase E at 3638 cm^{-1} is 2.694 Å, which is much longer than the limit of an ideal H-bond (2.4 Å) (Lutz et al., 1994). For such a higher frequency vibration in phase E we do not exclude the possibility of a strong H–H repulsive or van der Waals force.

For phase D, two partially occupied H sites were reported based on single-crystal XRD data and the O–H distances were 0.91 and 1.77 Å, respectively (Yang et al., 1997). In addition, the O···O distance was determined as 2.676 Å (Yang et al., 1997). In this study, six OH bands, 2120, 2240, 2461, 2850, 3160, and 3370 cm^{-1}, were observed. The IR band at 2850 cm^{-1} is close to previous Raman observations, 2847 cm^{-1} (Frost and Fei, 1998). We adopted the correlation of OH frequency with O···H and O···O bond distance from Libowitzky (1999) and calculated the O···H and O···O distances for phase D. Our results showed that the 2120, 2240, 2461, 2850, 3160, and 3370 cm^{-1} bands correspond to the H···O bond distances as 1.519, 1.536, 1.573, 1.660, 1.769, and 1.946 Å, and to the O···O distances as 2.225, 2.236, 2.260, 2.316, 2.691, and 2.817 Å. Note that the OH stretching at 3160 cm^{-1}, which is not well resolved from the Raman measurements (Frost and Fei, 1998), has a correlation of O···H bond length of 1.769 Å that is close to single-crystal X-ray measurements. Moreover, the associated O···O distance for 3160 cm^{-1} is 2.691 Å, which is also close to the single crystal X-ray measurement (Yang et al., 1997).

Using the correlation of O–H frequency with H···O and O···O distances (Libowitzky, 1999), we calculate the H···O and O···O distances for phase D to about 42 GPa. Our results show that the bond distance of H···O corresponding to the 3160 and 3370 cm^{-1} modes slowly decreases from 1.769 to 1.755 Å and from 1.946 to 1.854 Å. However, for the 2850 cm^{-1} band, the bond distance weakly increases from 1.660 to 1.692 Å. Our results for the O···O distance of phase D show that the 2850, 3160, and 3370 cm^{-1} bands have corresponding O···O bond distances that vary from 2.316 to 2.336 Å, 2.691 to 2.682 Å, and 2.817 to 2.750 Å, respectively, as pressure increases. In the case of the 3160 cm^{-1} band, the O···O bond distance decreases to 2.682 Å at ~42 GPa. Since the H···O bond distance at the same pressure is estimated as 1.755 Å, the O–H bond distance will be 0.927 Å, based on a linear O–H···O bond. However, it should be noted that the applicability of such empirical systematics for O–H···O bonds based on chemical variation at 1 bar may not be directly applicable to bond variation at high pressures as O–H frequencies may also be sensitive to other factors such as changes in the hydrogen potential (Nelmes et al., 1993; Winkler et al., 2008).

For phase E, the location and number of hydrogen sites remains unclear. For the four OH bands, 2455, 2988, 3411, and 3638 cm^{-1}, observed in this study, the corresponding H···O bond distances are 1.572, 1.702, 1.931, and 2.693 Å, and the O···O distances are 2.563, 2.647, 2.806, and 2.986 Å. The O···O bonding length determined from the single-crystal X-ray measurement is 2.860 Å (Kudoh et al., 1993), which is slightly higher than that of 2.806 Å at 3411 cm^{-1} band. As pressure increases to 41 GPa, the IR bands of phase E at 2988, 3411, and 3638 cm^{-1} have corresponding H···O distances of 1.672, 1.811, and 2.449 Å, whereas the corresponding O···O bond distances are 2.628, 2.720, and 3.096 Å, respectively. If we exclude the 3638 cm^{-1} band, the H···O bond distances of phase E reduce from the range of 1.572–1.931 Å to a narrower range of 1.579–1.811 Å. Similar reduction of bond distances can be also seen from the correlation O···O distances of phase E to 41 GPa.

3.4. Symmetrization of hydrogen bond

Hydrogen bond symmetrization in phase D has been predicted to occur near 40 GPa by first-principles calculation (Tsuchiya et al., 2005). In this process, the double well potential of the H atom evolves with pressure until a single minimum is reached and the H atom lies midway between the donor and acceptor oxygens. This transition is predicted to be accompanied by an increase in the bulk modulus of ~20% for phase D (Tsuchiya et al., 2005). Symmetric hydrogen bonding has been reported experimentally at high pressures in molecular solids such as H_2O, HBr, and HCl from Raman and infrared spectroscopic measurements that show the molecular stretching frequency decreasing to zero and the molecular stretching mode disappearing while lattice modes remain (Aoki et al., 1996, 1999; Goncharov et al., 1999). In addition to phase D, symmetrization has also been predicted to occur in the high-pressure phase of diaspore, δ-AlOOH (Tsuchiya et al., 2002) and the effect of symmetrization on vibrational frequencies has been calculated for this material (Tsuchiya and Tsuchiya, 2008).

Our IR measurements on phase D to 42 GPa do not show direct evidence for any of the expected changes in the OH stretching region that might accompany symmetrization. Specifically, we do not observe any dramatic changes in the frequency or intensity of OH stretching vibrations with increasing pressure. We also do not observe merging of the separate OH peaks into a single stretching

vibration (Tsuchiya and Tsuchiya, 2008), although extrapolation of our data suggests this could occur near 112 GPa. There also appears to be some weakening of intensity of the modes in the OH stretching region at the highest pressures (Fig. 2), and this might possibly be related to symmetrization at pressures beyond the range of this study. However, such weakening can also arise from sample thinning with compression. One possible explanation for the discrepancy between experiments and theoretical calculations may be attributed to the non-stoichiometric nature of phase D. Phase D possesses a non-stoichiometric chemical composition whereas Tsuchiya et al. (2005) used an ideal chemical composition (i.e., $MgSi_2O_4(OH)_2$) for their calculations. Therefore, the theoretical prediction of hydrogen symmetrization pressure may be underestimated. Also, the exact locations of the hydrogen in the structure are not well constrained and may differ from the assumptions made by Tsuchiya et al. (2005). There is a significant difference in the calculated bond lengths (O–H = 1.052 Å, H···O = 1.561 Å) (Tsuchiya et al., 2005) and the experimental values of Yang et al. (1997) (O–H = 0.91 Å, H···O = 1.766 Å). This may lead to an underestimate of the pressure at which these bond lengths will merge under compression.

A change in compression mechanism and increased bulk modulus is predicted to accompany symmetrization. In particular, it was proposed that the flattening of the crystallization c/a ratio observed around 20 GPa (Frost and Fei, 1999) could be a signature of symmetrization in phase D (Tsuchiya et al., 2005). However, flattening of the c/a ratio with compression is observed in other hydrous minerals such as phase E and various hydroxides (Kruger et al., 1989; Nguyen et al., 1994; Duffy et al., 1995; Shieh and Duffy, 2002; Shieh et al., 2000a,b) without any accompanying spectroscopic signature characteristic of symmetrization, so this is an ambiguous criterion.

4. Conclusions

The high-pressure IR spectra of phases D and E were observed for the first time in this study. No structural phase transition or amorphization was found for phases D and E to pressures up to ~40 GPa. The internal modes of frequency of phase D appear either higher than those of phase E at higher frequencies (>1000 cm^{-1}) or lower than those of phase E at lower frequencies (<900 cm^{-1}) as the nature of framework of phase D (SiO_6) is different from phase E (SiO_4) and both SiO_6 and SiO_4 are distorted. Moreover, the pressure-dependent frequency shifts of phase D are in general lower than those of phase E which can be attributed to the higher bulk modulus of phase D (K_T = 166 GPa) than that of phase E (K_T = 93 GPa). Using the correlations of OH frequency with H···O and O···O bond distances show that phase D has H···O and O···O bond distances in the range of 1.519–1.946 Å and 2.225–2.817 Å, whereas for the phase E has the H···O and O···O bond distances in the range of 1.562–2.693 Å and 2.557–2.986 Å. In addition, O···O bond distances obtained from the 3160 cm^{-1} band of phase D and 3411 cm^{-1} band for phase E are in agreement with single crystal data (Kudoh et al., 1993; Yang et al., 1997). Our high-pressure infrared measurements for phase D do not support the hydrogen bond symmetrization at about 40 GPa as suggested by first-principles calculation.

Acknowledgements

This work was supported by the NSF and the NSERC. We thank J. Konzett for assistance in the synthesis of phase E. Comments and suggestions from two anonymous reviewers helped to improve the quality of this work. Operation of beamline U2A at the NSLS is supported by COMPRES, the Consortium for Material Properties Research in the Earth Sciences under NSF Cooperative Agreement Grant No. EAR01-35554, and the U.S. Department of Energy (DOE) (CDAC, Contract No. DE-FC03-03N00144).

References

Aoki, K., Yamawaki, H., Sakashita, M., Fujihisa, H., 1996. Infrared absorption study of the hydrogen-bond symmetrization in ice to 110 GPa. Phys. Rev. B 54, 15673–15677.
Aoki, K., Katoh, E., Yamawaki, H., Sakashita, M., Fujihisa, H., 1999. Hydrogen-bond symmetrization and molecular dissociation in hydrogen halides. Phys. B 265, 83–86.
Cynn, H., Hofmeister, A.M., Burnley, P.C., Navrotsky, A., 1996. Thermodynamic properties and hydrogen speciation from vibrational spectra of dense hydrous magnesium silicates. Phys. Chem. Miner. 23, 361–367.
Duffy, T.S., Shu, J., Mao, H.K., Hemley, R.J., 1995. Single-crystal X-ray diffraction of brucite to 14 GPa. Phys. Chem. Miner. 22, 277–281.
Frost, D.J., 1999. The stability of dense hydrous magnesium silicates in Earth's transition zone and lower mantle. In: Fei, Y., Berka, C.M., Mysen, B.O. (Eds.), Mantle Petrology, Field Observation and High Pressure Experimentation, vol. 6. The Geochemical Society, pp. 283–296.
Frost, D.J., Fei, Y., 1998. Stability of phase D at high pressure and high temperature. J. Geophys. Res. 103, 7463–7474.
Frost, D.J., Fei, Y., 1999. Static compression of the hydrous magnesium silicate phase D to 30 GPa at room temperature. Phys. Chem. Miner. 26, 415–418.
Goncharov, A.F., Struzhkin, V.V., Mao, H.K., Hemley, R.J., 1999. Raman spectroscopy of dense H_2O and the transition to symmetric hydrogen bonds. Phys. Rev. Lett. 83, 1998–2001.
Hofmeister, A.M., Cynn, H., Burnley, P.C., Meade, C., 1999. Vibrational spectra of dense, hydrous magnesium silicates at high pressure: importance of the hydrogen bond angle. Am. Miner. 84, 454–464.
Irifune, T., Kubo, N., Isshiki, M., Yamasaki, Y., 1998. Phase transformations in serpentine and transportation of water into the lower mantle. Geophys. Res. Lett. 25, 203–206.
Jacobsen, S.D., van der Lee, S. (Eds.), 2006. Earth's Deep Water Cycle. Am. Geophys. Union, 314 pp.
Kanzaki, M., 1991. Stability of hydrous magnesium silicates in the mantle transition zone. Phys. Earth Planet. Inter. 66, 307–312.
Kawamoto, T., 2004. Hydrous phase stability and partial melt chemistry in H_2O-saturated KLB-1 peridotite up to the uppermost lower mantle conditions. Phys. Earth Planet. Inter. 143–144, 387–395.
Kleppe, A.K., Jephcoat, A.P., Ross, N.L., 2001. Raman spectroscopic studies of phase E to 19 GPa. Am Mineral. 86, 1275–1281.
Komabayashi, T., Omori, S., 2006. Internally consistent thermodynamic data set for dense hydrous magnesium silicate up to 35 GPa. 1600 °C: implication for water circulation in the Earth's deep mantle. Phys. Earth Planet. Int. 156, 89–107.
Kruger, M.B., Williams, Q., Jeanloz, R., 1989. Vibrational spectra of $Mg(OH)_2$ and $Ca(OH)_2$ under pressure. J. Chem. Phys. 91, 5910–5915.
Kudoh, Y., Finger, L.W., Hazen, R.M., Prewitt, C.T., Kanzaki, M., Veblen, D.R., 1993. Phase E: a high pressure hydrous silicate with unique crystal structure. Geophys. Res. Lett. 24, 1051–1054.
Kudoh, Y., Nagase, T., Mizohata, H., Ohtani, E., Sasaki, S., Tanaka, M., 1997. Structure and crystal chemistry of phase G, a new hydrous magnesium silicate synthesized at 22 GPa and 1050 °C. Phys. Chem. Miner. 19, 357–360.
Libowitzky, E., 1999. Correlation of O–H stretching frequencies and O–H···O hydrogen bond lengths in minerals. Monatshefte fur Chemie 130, 1047–1059.
Litasov, K., Ohtani, E., 2003. Stability of various hydrous phases in CMAS pyrolite–H_2O system up to 25 GPa. Phys. Chem. Miner. 30, 147–156.
Liu, L., 1986. Phase transformations in serpentine at high pressures and temperatures and implications for subducting lithosphere. Phys. Earth Planet. Inter. 42, 255–262.
Liu, L., 1987. Effects of H_2O on the phase behaviour of the forsterite–enstatite system at high pressures and temperatures and implications for the Earth. Phys. Earth Planet. Inter. 49, 142–147.
Liu, L.G., Lin, C.C., Irifune, T., Mernagh, T.P., 1998. Raman study of phase D at various pressures and temperatures. Geophys. Res. Lett. 25, 3453–3456.
Liu, Z., Lager, G.A., Hemley, R.J., Ross, N.L., 2003. Synchrotron infrared spectroscopy of OH-chondrodite and OH-clinohumite at high pressure. Am Miner. 88, 1412–1415.
Lutz, H.D., 1995. Hydroxide ions in condensed materials—correlation of spectroscopic and structural data. Struct. Bonding 82, 86–103.
Lutz, H.D., Beckenkamp, K., Moller, H., 1994. Weak hydrogen bonds in solid hydroxides and hydrates. J. Mol. Struct. 322, 263–266.
Mao, H.K., Bell, P.M., Shaner, J.W., Steinberg, D.J., 1978. Specific volume measurements of Cu, Mo, Pt and Au and calibration of ruby R1 fluorescence pressure gauge for 0. 06 to 1 Mbar. J. Appl. Phys. 49, 3276–3283.
Mernagh, T.P., Liu, L., 1998. Raman and infrared spectra of phase E: a plausible hydrous phase in the mantle. Can. Miner. 36, 1217–1223.
Nelmes, R.J., Loveday, J.S., Wilson, R.M., Besson, J.M., Pruzan, P., Klotz, S., Hamel, G., Hull, S., 1993. Neutron diffraction study of the structure of deuterated ice VIII to 10 GPa. Phys. Rev. Lett. 71, 1192–1195.
Nguyen, J.H., Kruger, M.B., Jeanloz, R., 1994. Compression and pressure-induced amorphization of $Co(OH)_2$ characterized by infrared vibrational spectroscopy. Phys. Rev. B 49, 3734–3738.

Ohtani, E., Shibata, T., Kudoh, T., Kato, T., 1995. Stability of hydrous phases in the transition zone and the upper most part of the lower mantle. Geophys. Res. Lett. 22, 2553–2556.
Ohtani, E., Mizobata, H., Kudoh, T., Nagase, T., Arashi, H., Yurimoto, H., Miyagi, I., 1997. A new hydrous silicate, a water reservoir, in the upper part of the lower mantle. Geophys. Res. Lett. 24, 1047–1050.
Ohtani, E., Toma, M., Litasov, K., Kubo, T., Suzuki, A., 2001. Stability of dense hydrous magnesium silicate phases and water storage capacity in the transition zone and lower mantle. Phys. Earth Planet. Inter. 124, 105–117.
Ohtani, E., Litasov, K., Hosoya, T., Kubo, T., Kondo, T., 2004. Water transport into the deep mantle and formation of a hydrous transition zone. Phys. Earth Planet. Inter. 143–144, 255–269.
Shieh, S.R., Duffy, T.S., 2002. Raman spectroscopy of $Co(OH)_2$ at high pressures: implications for amorphization and hydrogen repulsion. Phys. Rev. B, 134301.
Shieh, S.R., Duffy, T.S., 2003. High-pressure studies of hydrogen and carbon-bearing materials. EOS, American Geophysical Union (V31D0966S).
Shieh, S.R., Ming, L.C., 1996. The X-ray diffraction study of high pressure phase of serpentine. EOS, American Geophysical Union 77 (46), 682.
Shieh, S.R., Mao, H.K., Hemley, R.J., Ming, L.C., 1998. Decomposition of phase D at lower mantle and the fate of dense hydrous magnesium silicates in subducting slabs. Earth Planet. Sci. Lett. 159, 13–23.
Shieh, S.R., Mao, H.K., Kozett, J., Hemley, R.J., 2000a. In-situ high-pressure X-ray diffraction of phase E to 15 GPa. Am. Miner. 85, 765–769.
Shieh, S.R., Mao, H.K., Hemley, R.J., Ming, L.C., 2000b. In-situ X-ray diffraction studies of dense hydrous magnesium silicates at mantle conditions. Earth Planet. Sci. Lett. 177, 69–80.
Smyth, J.R., 2006. Hydrogen in high pressure silicate and oxide mineral structures. In: Water in Nominally Anhydrous Minerals. Rev. Miner. Geochem. 62, 85–115.
Stalder, R., Ulmer, P., 2001. Phase relations of a serpentine composition between 5 and 14 GPa: significance of clinohumite and phase E as water carriers into the transition zone. Contrib. Miner. Petrol. 140, 670–679.
Tsuchiya, J., Tsuchiya, T., Tsuneyuki, S., Yamanaka, T., 2002. First principles calculation of a high-pressure hydrous phase, δ-AlOOH. Geophys. Res. Lett. 29, 1909, doi:10.1029/2002GL015417.
Tsuchiya, J., Tsuchiya, T., Tsuneyuki, S., 2005. First-principles study of hydrogen bond symmetrization of phase D under high pressure. Am. Miner. 90, 44–49.
Tsuchiya, J., Tsuchiya, T., 2008. Elastic properties of phase D (MgSi2O6H2) under pressure: ab initio investigation. Phys. Earth Planet. Inter. 170 (215-220), 2008.
Williams, Q., 1992. A vibrational spectroscopic study of hydrogen in high pressure mineral assemblages. In: Syono, Y., Manghnani, M.H. (Eds.), High-Pressure Research: Application to Earth and Planetary Sciences. American Geophysical Union, Washington, DC, pp. 289–296.
Williams, Q., Guenther, L., 1996. Pressure-induced changes in the bonding and orientation of hydrogen in FeOOH-goethite. Solid State Commun. 100, 105–109.
Williams, Q., Hemley, R.J., 2001. Hydrogen in the deep Earth. Annu. Rev. Earth Planet. Sci. 29, 365–418.
Winkler, B., Gale, J.D., Refson, K., Wilson, D.J., Milman, V., 2008. The influence of pressure on the structure and dynamics of hydrogen bonds in zoisite and clinozoisite. Phys. Chem. Miner. 35, 25–35.
Wood, B.J., Corgne, A., 2007. Trace elements and volatiles in the deep Earth. In: Schubert, G. (Ed.), Treatise on Geophysics, vol. 2. Elsevier, pp. 63–89.
Xue, X., Kanzaki, M., Shatskiy, A., 2008. Dense hydrous magnesium silicates, phase D, and superhydrous B: new structural constraints from one- and two-dimensional ^{29}Si and ^{1}H NMR. Am. Miner. 93, 1099–1111.
Yang, H., Prewitt, C.T., Frost, D.J., 1997. Crystal structure of the dense hydrous magnesium silicate, phase D. Am. Miner. 82, 651–654.